Modeling of the Optimal Trajectory Control System of Constant Frequency Series Resonant Converter

Nikolay Bankov[1] and Aleksandar Vuchev[2]

Abstract – **An optimal trajectory control system (CS) of series resonant converter (SRC) operating at constant frequency (CF) above the resonant one is proposed. CS is designed on the base of state-plane analysis of SRC and is realized on the principle of the Analog Behavioral Modeling, set in the OrCAD PSpice simulator. The aim is to determine the time intervals in the commutation process when the oscillating circuit voltage and current alter according to an optimal trajectory. This approach gives the opportunity to obtain minimum response time at guaranteed stable converter operation.**

Keywords – **Resonant DC/DC converters, Control system, Optimal trajectory control, Behavioural modelling.**

I. Introduction

In the recent years, different methods for control of series resonant converters (SRC) operating above the resonant frequency have been widely discussed and compared [1, 2]. One of them is the method for optimal control of the desired converter operation trajectory. Advantages of the considered optimal control method compared to the other control methods are reduction of the reactive and switching circuit components voltage stresses, as well as, fast dynamic response in case of large variations in the operating conditions at guaranteed stable converter operation.

By the state-plane analysis, accurate description of the converter operation in static and dynamic mode is obtained [2]. On the base of this analysis, optimal trajectory control of SRC is presented for both variable [3] and constant frequency [4].

In [4], block-diagram of optimal trajectory control system (CS) of SRC operating at constant frequency above the resonant is presented.

Deeper investigations are presented in the following paperwork as a particular version of CS is proposed realized on the principle of Analog Behavioral Modeling by the means of the OrCAD PSpice simulator.

The obtained results are presented and analyzed evidencing proper converter operation accomplished by optimal trajectory control.

[1]Nikolay Bankov is with the Department of Electrical Engineering and Electronics, Technical Faculty, University of Food Technologies, 26 Maritza Blvd., 4002 Plovdiv, Bulgaria, E-mail: nikolay_bankov@yahoo.com

[2]Aleksandar Vuchev is with the Department of Electrical Engineering and Electronics, Technical Faculty, University of Food Technologies, 26 Maritza Blvd., 4002 Plovdiv, Bulgaria, E-mail: avuchev@yahoo.com

II. State-Plane Analysis of CF-SRC

The circuit of the examined converter is presented in Fig. 1. For the analysis purposes, the following assumptions are made: the switches are ideal and have zero switching time; the resonant tank quality factor is infinitely large; the filter capacitor C_0 has significant capacitance so that the output voltage remains constant within several commutation cycles. Switches $Q1$ and $Q3$ commutate at constant frequency (f_S), receiving control signals with duty cycle of 50%. Switches $Q2$ and $Q4$ are switched on and off by signals with the same steady-state frequency as the one for $Q1$ and $Q3$ but phase shifted, so that $Q2$ (Q4) switch on before $Q1$ (Q3). The operating frequency is above the resonant one.

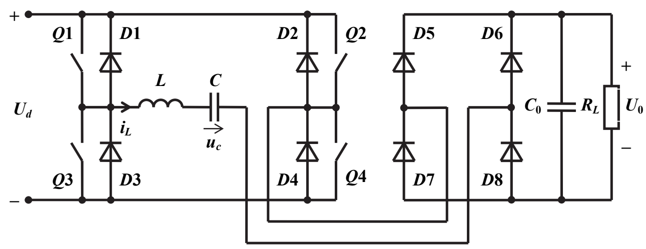

Fig. 1. CF-SRC Configuration

At deep variation of the load and the phase shift between the control pulses, two different operating modes of the converter can be observed. They are illustrated in Fig. 2 and Fig. 3 with the state trajectory in the state plane $\left(x = U'_C ; y = I'_L\right)$. For each conduction interval of the power switches and the freewheeling diodes, ark from a circle is drawn with radius determined by the initial values of the capacitor voltage U'_{C0} and current I'_{L0} and center (U'_0, 0), (1+U'_0, 0), (1-U'_0, 0) or the mirror images of these points with respect to the I'_L axis. It should be emphasized that all the magnitudes in the phase plane are normalized – voltages with respect to the supply voltage U_d, currents with respect to the current factor $U_d / \sqrt{L/C}$.

In Fig. 2, the transition from the conduction interval of $Q1$-$D2$ to the interval $D2$-$D3$ and from $Q3$-$D4$ to $D1$-$D4$ is realized by the switching of $Q1$ and $Q3$ with constant frequency. In Fig. 3, the transition from the interval $Q4$-$D3$ to $Q1$-$Q4$ and from $Q2$-$D1$ to $Q3$-$Q2$ is realized by switching of $Q1$ and $Q3$ with constant frequency. In both the two figures, the transition from $Q1$-$Q4$ to $Q1$-$D2$ and from $Q2$-$Q3$ to $Q3$-$D4$ is obtained by switching of $Q2$ and $Q4$.

After the switching of $Q2$ ($Q4$), the interval $Q1$-$D2$ ($Q3$-$D4$) begins, describing ark of a circle with radius R and centre (-U'_0, 0) or (+U'_0, 0).

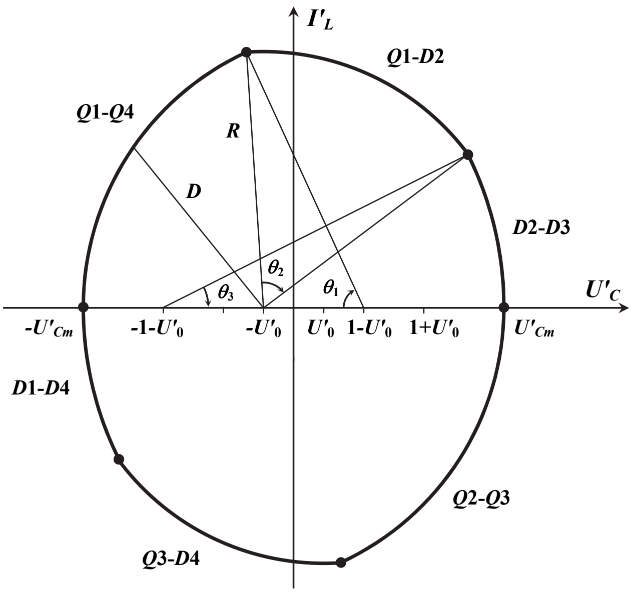

Fig. 2. State-plane Trajectory-Mode1

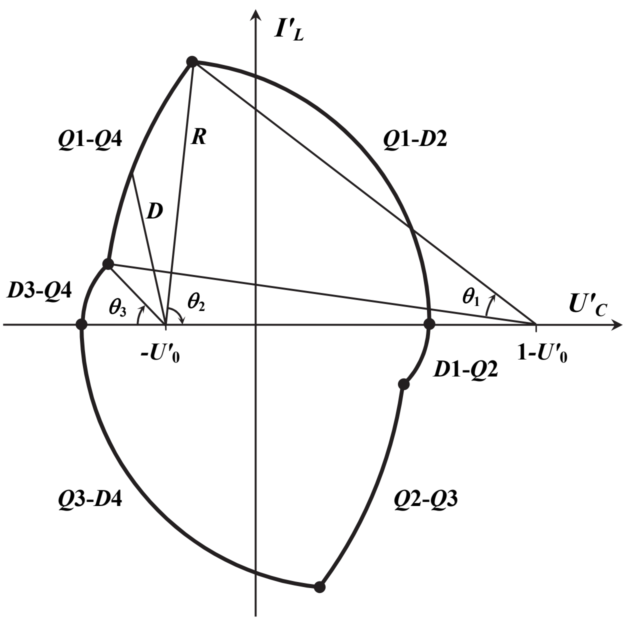

Fig. 3. State-plane Trajectory-Mode2

The parameter R characterises the converter resonant tank “momentary” energy. Therefore, it can be used as a parameter for control of the energy transfer between the power supply, the oscillating circuit and the load in a way similar to the one used in [2]. Such direct control of the resonant tank energy leads to reduction of the transient processes time and fast settling of the inductor current and the switching capacitor voltage at optimal trajectory.

The aim of the optimal trajectory control is to determine the moments of switching of $Q2$ and $Q4$ which accelerate the settling of the capacitor voltage and the inductor current at optimal trajectory for the given operating mode. In this way, the duration of the transient processes is minimized and steady state is achieved for short period of time. For this purpose, when the converter operates in the interval Q1-Q4 (Q2-Q3), the distance D measured from the center ($-U'_0$, 0) or ($+U'_0$, 0) to the trajectory is constantly observed, and when it equals the parameter R desired value, switches Q2(Q4) commutate.

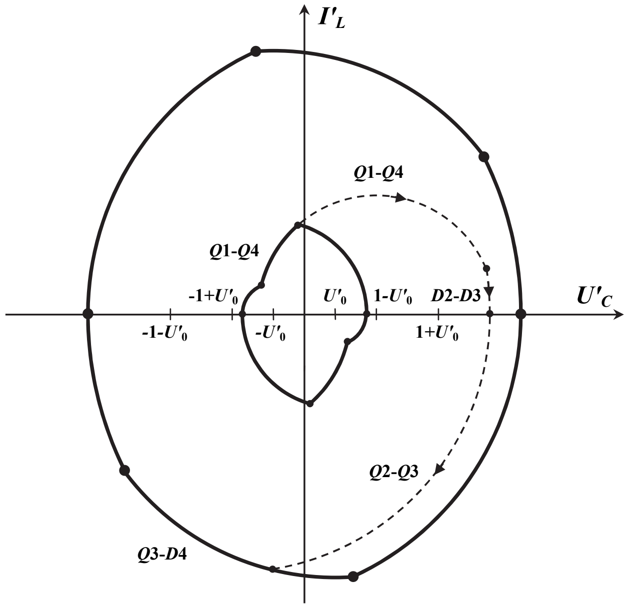

Fig. 4. Transition from a small to a large value of the parameter R

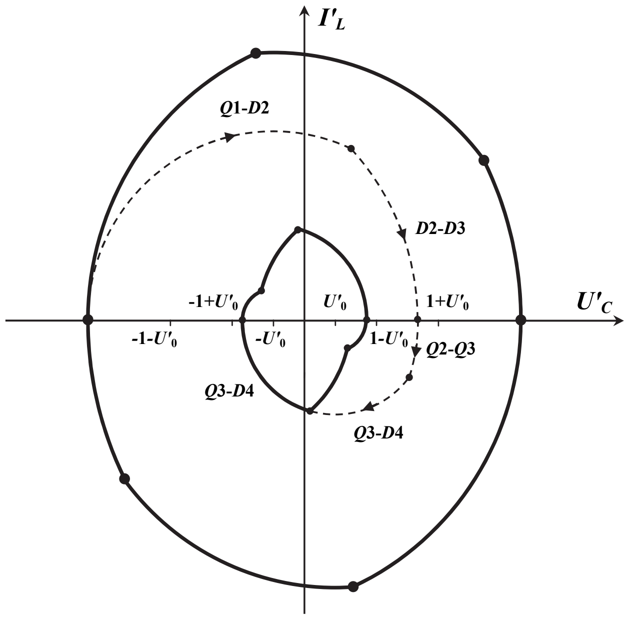

Fig. 5. Transition from a large to a small value of the parameter R

In the conduction interval of $Q1$-$Q4$, the distance D is determined by:

$$D = \sqrt{\left(U'_C + U'_0\right)^2 + I'^2_L} \tag{1}$$

In the conduction interval of $Q2$-$Q3$, the expression for D is:

$$D = \sqrt{\left(U'_C - U'_0\right)^2 + I'^2_L} \tag{2}$$

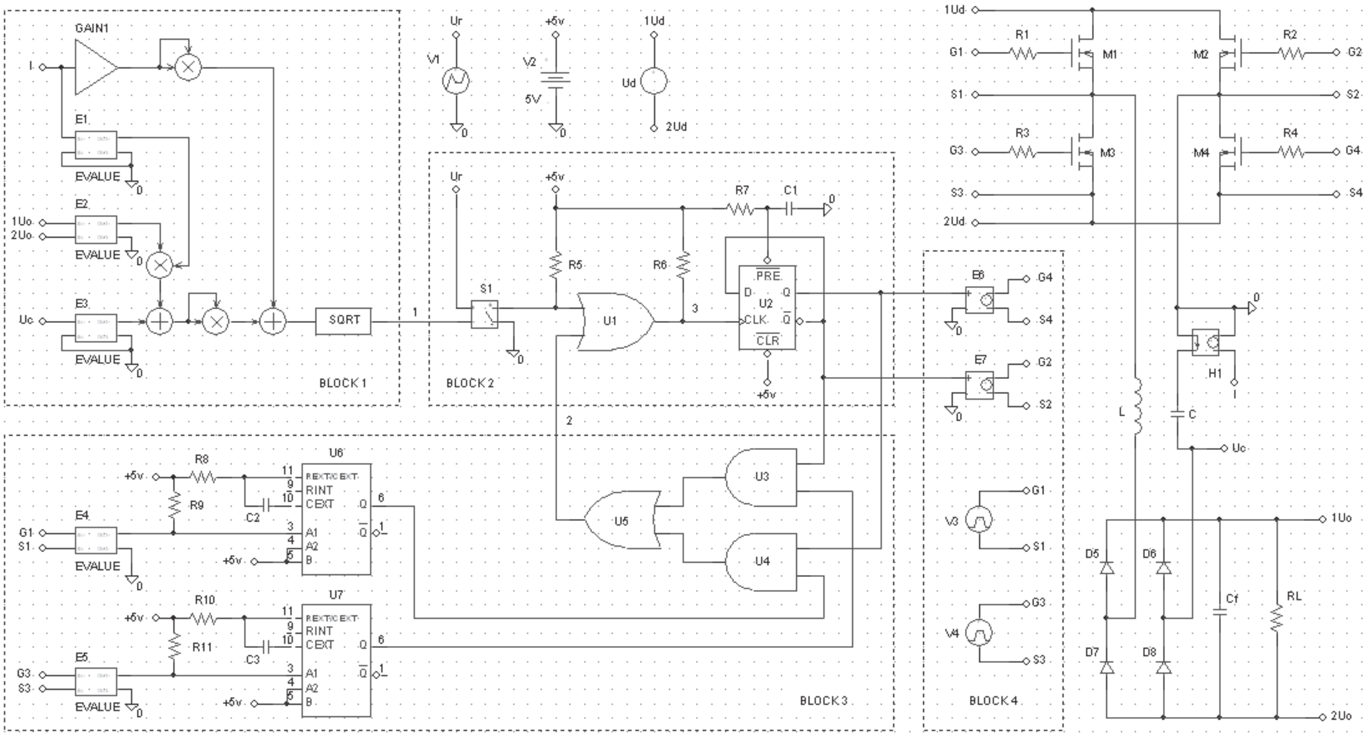

Fig. 6. Converter control system

In this way, the switching of $Q2$ and $Q4$ can be determined by:

$$R \le \sqrt{\left(U'_C \pm U'_0\right)^2 + I'^2_L} \quad (3)$$

The plus sign (+) corresponds to the first half period when $I'_L>0$, and the minus sign (-) – to the second half period at $I'_L<0$.

The transient processes at intermittent increase or decrease of the parameter R are shown in Fig. 4 and Fig. 5, respectively. The figures also present the power switches commutation sequence at optimal trajectory control. It can be observed that in both of the cases the transient processes duration is less than a period.

The commutation of the switches $Q2$ and $Q4$, as it has been described, happens at $D=R$. During the transition from a small to a large value of the parameter R, $D<R$. Then, $Q2$ and $Q4$ switch together with $Q1$ and $Q3$ ($\theta_2 = 0$) to $D=R$ (Fig. 4). In this way, the resonant circuit energy has the fastest increase.

During the transition from a large to a small value of the parameter R, $D>R$ and $Q2$ and $Q4$ switch immediately. The interval $Q1$-$Q4$ ($Q2$-$Q3$) is shortened or completely disappears, and intervals $Q1$-$D2$ ($Q3$-$D4$) and $D2$-$D3$ ($D1$-$D4$) are extended to $D=R$ (Fig. 5). Thus, the resonant circuit energy has the fastest decrease.

III. Control System

CS of the converter is realized on the principle of theAnalog Behavioral Modeling set in the PSPICE A/D simulator [5]. This approach allows versatile description of the electronic components on the base of transfer function or tabular assignments. In other words, instead of real components for modelling of circuit parts, their mathematical description is applied. With this, a combination of significant calculation efficiency and adequate component modelling is achieved.

The converter circuit, as well as, its control system are presented in Fig.6. MOSFET transistors are used as switching elements.

The distance D from the point that characterizes the resonant circuit state to the commutation center in relative units has the following form:

$$D = \sqrt{\left(U'_C + \operatorname{sgn} I'_L \cdot U'_0\right)^2 + I'^2_L} \quad (4)$$

The distance D is calculated by BLOCK1 as follows: the information for the resonant tank current is obtained via a current controlled subordinate voltage source H1. The signals for the output voltage and the switching capacitor voltage are sent to voltage controlled subordinate voltage sources EVALUE (E2 and E3). The current sign ($\operatorname{sgn} I'_L$) is obtained via voltage controlled subordinate voltage sources EVALUE E1 which realizes the following function:

$$\text{SGN(V(\%IN+, \%IN-))} \quad (5)$$

The obtained value for D (the BLOCK1 output) is sent to BLOCK2 for comparison with the reference Ur. The pulses formed by the comparator S1 and the logic element U1 are submitted to the latch U2. It forms two channels of pulses phase shifted at 180° for control of the switches $Q2$ and $Q4$.

The forced increase of the resonant circuit energy at $\theta_2 = 0$ (Fig.4) is realized by BLOCK3 which contains the voltage controlled subordinate voltage sources EVALUE (E4 and E5), monostable multivibrators 74121 (U6 and U7), as well as, logic elements U3, U4 and U5.

BLOCK4 contains pulse voltage sources V3 and V4 for constant frequency control of *Q*1 and *Q*3, as well as, controlled voltage sources E6 and E7 which provide the necessary power, magnitude and galvanic isolation of the control signals for *Q*2 and *Q*4.

The operation of the resonant converter CS is illustrated by the waveforms in Fig. 7.

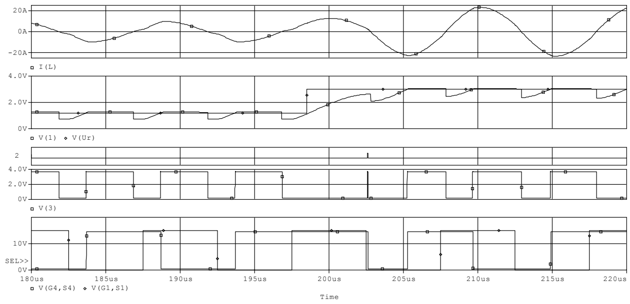

Fig. 7. Control system main waveforms.

Figs. 8, 9 and 10 presents results from the computer simulations with OrCAD PSpice, as the converter response is examined at significant variation of the control signal. Fig. 8 presents the converter start-up at R = 3.0, Fig. 9 and Fig. 10 illustrate the converter operation at intermittent alteration of the control system input signal - from R = 1.2 to R= 3.0 and respectively from R = 3.0 to R= 1.2.

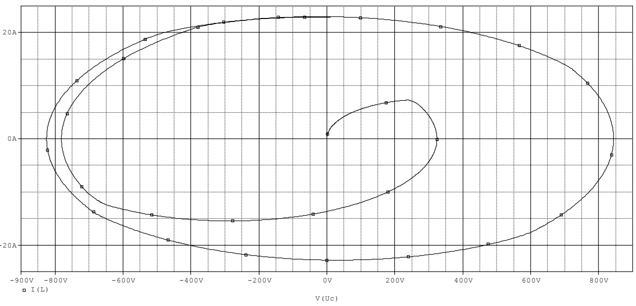

Fig. 8. Converter start-up R = 3.0

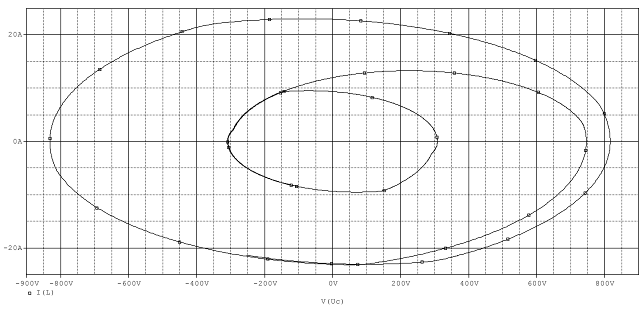

Fig. 9. Response of optimal trajectory control for Control increase $R = 1.2 \rightarrow R= 3.0$

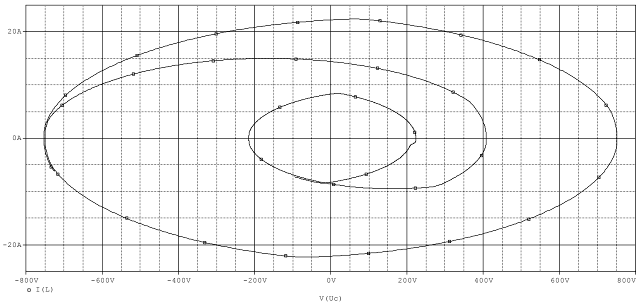

Fig. 10. Response of optimal trajectory control for Control decrease $R = 3.0 \rightarrow R= 1.2$

At start-up (Fig. 8), the initially gained resonant circuit energy is zero, and at R = 1.2 (Fig. 9) its value is very small. During the transition to R = 3.0, only the energy accumulation stage exists, whereat the two power switch commutate without phase shift between them.

In the other case (Fig. 10), beginning at the steady state at R = 3.0, the value of the accumulated resonant tank energy is too large. This forces one of the power switch couples to switch off, ceasing in this way the energy accumulation in the resonant circuit.

In all the three cases, the system reaches the steady trajectory for the minimum possible time, which is restricted only by the resonant converter features. From the figures, the stable converter operation with optimal trajectory control can be observed.

IV. CONCLUSION

A control method for series-resonant DC-DC converter operating at constant frequency above the resonant is considered. Computer models of the converter and the optimal trajectory control system realized in the environment of OrCAD PSpice are presented.

The simulation results show a very good dynamic response and steady converter operation.

The obtained results can be used for design and practical realization of resonant DC-DC converters using the considered optimal trajectory control.

REFERENCES

[1] Y. Cheron, H. Foch, and J. Roux, "Power Transfer Control Methods in High Frequency Resonant Converters", *PCI Proceedings*, June 1986, Munich, pp. 92-103.

[2] R. Oruganti, and F.C. Lee, "Resonant Power Processor: Part II - Methods of Control", *Proc. IEEE-IAS'84 Ann. Meet.*, pp. 868-878, 1984.

[3] N. Bankov, Ts. Grigorova, "Load Characteristics and Control System Behavioral Modeling Under Optimal Trajectory Control of Series Resonant DC/DC Converters", *Journal of Electrical Engineering*, vol. 56, No. 9-10, 2005, 258-264.

[4] K. Natarajan, and S. Sivakumar, "Optimal Trajectory Control of Constant Frequency Series Resonant Converter", *24th Annual IEEE Power Electronics Specialists Conference PESC '93*, pp. 215-221, June 1993.

[5] *OrCAD PSpice A/D User's Guide*, OrCAD Inc., USA, 1999.